

# Experiments in Quasi-Static Manipulation of a Planar Elastic Rod

Dennis Matthews and Timothy Bretl

**Abstract**—In this paper, we introduce and experimentally validate a sampling-based planning algorithm for quasi-static manipulation of a planar elastic rod. Our algorithm is an immediate consequence of deriving a global coordinate chart of finite dimension that suffices to describe all possible configurations of the rod that can be placed in static equilibrium by fixing the position and orientation of each end. Hardware experiments confirm this derivation in the case where the “rod” is a thin, flexible strip of metal that has a fixed base and that is held at the other end by an industrial robot. We show an example in which a path of the robot that was planned by our algorithm causes the metal strip to move between given start and goal configurations while remaining in quasi-static equilibrium.

## I. INTRODUCTION

Figure 1 shows a thin, flexible strip of metal that has a fixed base and that is held at the other end by an industrial robot. The problem we consider in this paper is to find a path of the robot that causes the metal strip to move between start and goal configurations while remaining in static equilibrium and avoiding self-collision. We view this problem equivalently as finding a path of the metal strip through its set of equilibrium configurations (i.e., the set of all configurations that would be in equilibrium if both ends of the metal strip were held fixed).

Our main contribution is to show that this set of equilibrium configurations is a smooth manifold of dimension three that can be parameterized by a single (global) coordinate chart. We proceed by modeling the metal strip as a planar elastic rod. Any curve traced by this rod in static equilibrium is a local solution to a geometric optimal control problem, with boundary conditions that vary with the placement of the robot. Coordinates for the set of *all* local solutions over *all* boundary conditions are provided by the initial value of costates that arise in necessary and sufficient conditions for optimality. These coordinates describe all configurations of the rod that can be achieved by quasi-static manipulation, and make the application of a sampling-based algorithm for manipulation planning straightforward and easy to implement.

Our paper is in many ways a response to the seminal work of Lamiroux and Kavraki [1] on manipulation of elastic objects, which was applied by Moll and Kavraki [2] to “deformable linear objects” like the planar elastic rod we consider here. This previous work clearly states that the set of equilibrium configurations is the space through which one *should* construct a manipulation plan. However, it ultimately suggests exploring this set indirectly, by sampling

D. Matthews is with the Department of Electrical and Computer Engineering and T. Bretl is with the Department of Aerospace Engineering, University of Illinois at Urbana-Champaign, Urbana, IL, 61801, USA {matthws1, tbretl}@illinois.edu

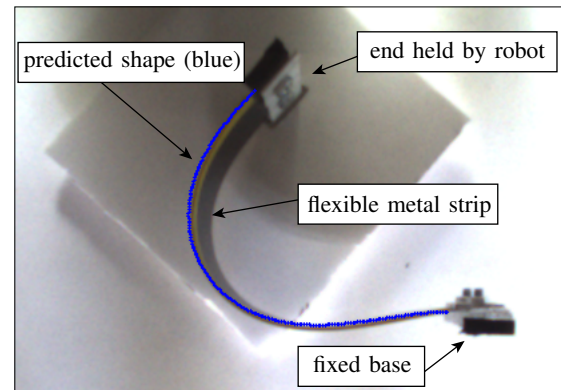


Fig. 1. Quasi-static manipulation of a thin, flexible strip of metal that has a fixed base and that is held at the other end by an industrial robot (view from below). The blue curve is the shape predicted by our model.

displacements of the robot and using numerical simulation to approximate their effect on the rod. It takes this approach for two reasons. First, the configuration space of the rod has infinite dimension. Elements of this space are continuous maps  $q: [0, 1] \rightarrow SE(2)$ , the shape of which in general must be approximated. Second, a countable number of configurations may be in static equilibrium for a given placement of the robot, none of which (typically) can be computed in closed form. For these two reasons, it seems hopeless to think that we might explicitly construct and parameterize the set of equilibrium configurations. In fact, doing so is indeed possible, as we will proceed to show.

The planar elastic rod has received a considerable amount of recent attention from Sachkov [3], [4], whose text on geometric optimal control (with Agrachev [5]) provides the basis for our own approach. Using Jacobi elliptic functions, this previous work derives a closed-form expression for the curve traced by a planar elastic rod in static equilibrium. It also gives either an exact description of or bounds on the location of conjugate points, cut points, and Maxwell points, which characterize local and global stability. This previous work does not answer our questions about the set of equilibrium configurations (is it a finite-dimensional manifold, what are its coordinate charts, etc.), but does provide formulae that could have replaced some of the computations we ultimately require for manipulation planning. We chose not to use these formulae because the computations we derive are trivial to implement and extend directly to the spatial case (i.e., to elastic rods that are not confined to the plane).

Although our contribution is primarily theoretical and our experiments are proof-of-concept, we are nonetheless motivated by applications that include knot tying and surgical

suturing [6]–[10], cable routing [11], folding clothes [12], compliant parts handling and assembly [13]–[15], surgical retraction of tissue [16], and protein folding [17]. We are also motivated by haptic exploration with “whisker” sensors, often modeled as elastic rods [18]. The coordinates we derive for equilibrium configurations have a direct interpretation as measured forces and torques, and may provide exactly the space in which to perform inference. Finally, we are motivated by the link, pointed out by Tanner [19], between manipulation of deformable objects and control of hyper-redundant [20] and continuum [21] robots. The coordinates we derive are an alternative to working either in the task space [22] or in the space of modal shapes derived from a heuristic choice of basis functions [23]. Similar ideas have been applied to dynamic redundancy resolution [24].

Section II establishes our theoretical framework. The two key parts of this framework are optimal control on manifolds and Lie-Poisson reduction. We derive coordinate formulae for necessary and sufficient conditions—in the former case these formulae are well known, but in the latter case they are not. Section III shows how our framework applies to the planar elastic rod. We prove that the set of equilibrium configurations for this rod is a smooth manifold of dimension three that can be parameterized by a single chart, and we present a sampling-based planning algorithm for quasi-static manipulation based on this result. Section IV validates our approach with hardware experiments, in which the “rod” is a flexible strip of metal that is held by an industrial robot. Section V concludes with opportunities for future work. Our ideas here follow from but significantly extend earlier work on a simpler model (a planar elastic kinematic chain [25]).

## II. THEORETICAL FRAMEWORK

We will see in Section III that the framed curve traced by a planar elastic rod in equilibrium is a local solution to a geometric optimal control problem. Here, we provide the framework to characterize this solution. This framework essentially relies on a geometric statement of Pontryagin’s maximum principle [26]. Section II-A states necessary and sufficient conditions for optimality on manifolds. Section II-B derives coordinate formulae to test these conditions. These results are a translation of [5] in a style more consistent with [27], [28]. We conclude with coordinate formulae to test sufficiency for left-invariant systems on Lie groups (Theorem 4), a result that is not in [5] and is hard to find elsewhere.

In what follows, we denote the space of all smooth real-valued functions on a smooth manifold  $M$  by  $C^\infty(M)$ . We also recall that a smooth map  $F: M \rightarrow N$  between smooth manifolds  $M$  and  $N$  is degenerate at  $m \in M$  if the Jacobian matrix of any coordinate representation of  $F$  at  $m$  has zero determinant. We use  $T_m F$  and  $T_m^* F$  to denote the pushforward and pullback of  $F$ , respectively. The rest of our notation is standard [28], [29].

### A. Optimal Control on Manifolds

Let  $M$  be a smooth manifold and let  $U \subset \mathbb{R}^m$  for some  $m > 0$ . Assume  $g: M \times U \rightarrow \mathbb{R}$  and  $f: M \times U \rightarrow TM$  are

smooth maps. Consider the optimal control problem

$$\begin{aligned} & \underset{q,u}{\text{minimize}} && \int_0^1 g(q(t), u(t)) dt \\ & \text{subject to} && \dot{q}(t) = f(q(t), u(t)) \text{ for all } t \in [0, 1] \\ & && q(0) = q_0, \quad q(1) = q_1, \end{aligned} \quad (1)$$

where  $q_0, q_1 \in M$  and  $(q, u): [0, 1] \rightarrow M \times U$ . Define the parameterized Hamiltonian  $\widehat{H}: T^*M \times \mathbb{R} \times U \rightarrow \mathbb{R}$  by

$$\widehat{H}(p, q, k, u) = \langle p, f(q, u) \rangle - kg(q, u),$$

where  $p \in T_q^*M$ .

*Theorem 1 (Necessary Conditions):* Suppose

$$(q_{\text{opt}}, u_{\text{opt}}): [0, 1] \rightarrow M \times U$$

is a local optimum of (1). Then, there exists  $k \geq 0$  and an integral curve  $(p, q): [0, 1] \rightarrow T^*M$  of the time-varying Hamiltonian vector field  $X_H$ , where  $H: T^*M \times \mathbb{R} \rightarrow \mathbb{R}$  is given by

$$H(p, q, t) = \widehat{H}(p, q, k, u_{\text{opt}}(t)),$$

that satisfies  $q(t) = q_{\text{opt}}(t)$  and

$$H(p(t), q(t), t) = \max_{u \in U} \widehat{H}(p(t), q(t), k, u) \quad (2)$$

for all  $t \in [0, 1]$ . If  $k = 0$ , then  $p(t) \neq 0$  for all  $t \in [0, 1]$ .

*Proof:* See Theorem 12.10 of [5]. ■

The integral curve  $(p, q)$  in Theorem 1 is an *abnormal extremal* when  $k = 0$  and a *normal extremal* otherwise. As usual, when  $k \neq 0$  we may assume  $k = 1$ . We call  $(q, u)$  abnormal if it is the projection of an abnormal extremal. We call  $(q, u)$  normal if it is the projection of a normal extremal and it is not abnormal.

*Theorem 2 (Sufficient Conditions):* Suppose

$$(p, q): [0, 1] \rightarrow T^*M$$

is a normal extremal of (1). Define  $H \in C^\infty(T^*M)$  by

$$H(p, q) = \max_{u \in U} \widehat{H}(p, q, 1, u), \quad (3)$$

assuming that the maximum exists and that  $\partial^2 \widehat{H} / \partial u^2 < 0$ . Define  $u: [0, 1] \rightarrow U$  so that  $u(t)$  is the unique maximizer of (3) at  $(p(t), q(t))$ . Assume that  $X_H$  is a complete vector field and that there exists no other integral curve  $(p', q')$  of  $X_H$  satisfying  $q(t) = q'(t)$  for all  $t \in [0, 1]$ . Let  $\varphi: \mathbb{R} \times T^*M \rightarrow T^*M$  be the flow of  $X_H$  and define the endpoint map  $\phi_t: T_{q(0)}^*M \rightarrow M$  by  $\phi_t(w) = \pi \circ \varphi(t, w, q(0))$ . Then,  $(q, u)$  is a local optimum of (1) if and only if there exists no  $t \in (0, 1]$  for which  $\phi_t$  is degenerate at  $p(0)$ .

*Proof:* See Theorem 21.8 of [5]. ■

### B. Lie-Poisson Reduction

Let  $G$  be a Lie group with identity element  $e \in G$ . Let  $\mathfrak{g} = T_e G$  and  $\mathfrak{g}^* = T_e^* G$ . Denote the functional derivative of any  $h \in C^\infty(\mathfrak{g}^*)$  at  $\mu \in \mathfrak{g}^*$  by  $\delta h / \delta \mu \in \mathfrak{g}$ , as in [28].

*Theorem 3 (Reduction of Necessary Conditions):* Let

$$H: T^*G \times [0, 1] \rightarrow \mathbb{R}$$

be both smooth and left-invariant for all  $t \in [0, 1]$ . Denote the restriction of  $H$  to  $\mathfrak{g}^*$  by  $h = H|_{\mathfrak{g}^* \times [0,1]}$ . Given  $p_0 \in T_{q_0}^*G$ , let  $\mu: [0, 1] \rightarrow \mathfrak{g}^*$  be the solution of

$$\dot{\mu} = \text{ad}_{\delta h / \delta \mu}^*(\mu) \quad (4)$$

with initial condition  $\mu(0) = T_e^*L_{q_0}(p_0)$ . The integral curve  $(p, q): [0, 1] \rightarrow T^*G$  of the time-varying Hamiltonian vector field  $X_H$  with initial condition  $p(0) = p_0$  satisfies

$$p(t) = T_{q(t)}^*L_{q(t)^{-1}}(\mu(t))$$

for all  $t \in [0, 1]$ , where  $q$  is the solution of

$$\dot{q} = X_{\delta h / \delta \mu}(q)$$

with initial condition  $q(0) = q_0$ .

*Proof:* See Theorem 13.4.4 of [28]. ■

It is convenient for us to introduce coordinates on  $\mathfrak{g}$  and  $\mathfrak{g}^*$ . Let  $\{X_1, \dots, X_n\}$  be a basis for  $\mathfrak{g}$  and let  $\{P_1, \dots, P_n\}$  be the dual basis for  $\mathfrak{g}^*$ . We write  $\zeta_i$  to denote the  $i$ th component of  $\zeta \in \mathfrak{g}$  with respect to this basis, and so forth. Define the structure constants  $C_{ij}^k \in \mathbb{R}$  by

$$[X_i, X_j] = \sum_{k=1}^n C_{ij}^k X_k \quad (5)$$

for  $i, j \in \{1, \dots, n\}$ . We require two lemmas before our main result (Theorem 4).

*Lemma 1:* Let  $q: U \rightarrow G$  be a smooth map, where  $U \subset \mathbb{R}^2$  is simply connected. Denote its partial derivatives  $\zeta: U \rightarrow \mathfrak{g}$  and  $\eta: U \rightarrow \mathfrak{g}$  by

$$\begin{aligned} \zeta(t, \epsilon) &= T_{q(t, \epsilon)}L_{q(t, \epsilon)^{-1}}\left(\frac{\partial q(t, \epsilon)}{\partial t}\right) \\ \eta(t, \epsilon) &= T_{q(t, \epsilon)}L_{q(t, \epsilon)^{-1}}\left(\frac{\partial q(t, \epsilon)}{\partial \epsilon}\right). \end{aligned} \quad (6)$$

Then,

$$\partial \zeta / \partial \epsilon - \partial \eta / \partial t = [\zeta, \eta]. \quad (7)$$

Conversely, if there exist smooth maps  $\zeta$  and  $\eta$  satisfying (7), then there exists a smooth map  $q$  satisfying (6).

*Proof:* See Proposition 5.1 of [30]. ■

*Lemma 2:* Let  $\alpha, \beta, \gamma \in \mathfrak{g}$  and suppose  $\gamma = [\alpha, \beta]$ . Then

$$\gamma_k = \sum_{r=1}^n \sum_{s=1}^n \alpha_r \beta_s C_{rs}^k.$$

*Proof:* This result follows from the definition (5). ■

*Theorem 4 (Reduction of Sufficient Conditions):* Assume that the Hamiltonian function  $H \in C^\infty(T^*G)$  is left-invariant and that the Hamiltonian vector field  $X_H$  is complete. Let  $h = H|_{\mathfrak{g}^*}$  be the restriction of  $H$  to  $\mathfrak{g}^*$  and let  $\varphi: \mathbb{R} \times T^*G \rightarrow T^*G$  be the flow of  $X_H$ . Given  $q_0 \in G$ , define the endpoint map  $\phi_t: T_{q_0}^*G \rightarrow G$  by  $\phi_t(p) = \pi \circ \varphi(t, p, q_0)$ . Given  $p_0 \in T_{q_0}^*G$ , let  $a \in \mathbb{R}^n$  be the coordinate representation of  $T_e^*L_{q_0}(p_0)$ , i.e.,

$$T_e^*L_{q_0}(p_0) = \sum_{i=1}^n a_i P_i. \quad (8)$$

Solve the ordinary differential equations

$$\dot{\mu}_i = - \sum_{j=1}^n \sum_{k=1}^n C_{ij}^k \frac{\delta h}{\delta \mu_j} \mu_k \quad i \in \{1, \dots, n\} \quad (9)$$

with the initial conditions  $\mu_i(0) = a_i$ . Define matrices  $\mathbf{F}, \mathbf{G}, \mathbf{H} \in \mathbb{R}^{n \times n}$  as follows:

$$[\mathbf{F}]_{ij} = - \frac{\partial}{\partial \mu_j} \sum_{r=1}^n \sum_{s=1}^n C_{ir}^s \frac{\delta h}{\delta \mu_r} \mu_s$$

$$[\mathbf{G}]_{ij} = \frac{\partial}{\partial \mu_j} \frac{\delta h}{\delta \mu_i}$$

$$[\mathbf{H}]_{ij} = - \sum_{r=1}^n \frac{\delta h}{\delta \mu_r} C_{rj}^i.$$

Solve the (linear, time-varying) matrix differential equations

$$\dot{\mathbf{M}} = \mathbf{F}\mathbf{M} \quad (10)$$

$$\dot{\mathbf{J}} = \mathbf{G}\mathbf{M} + \mathbf{H}\mathbf{J} \quad (11)$$

with initial conditions  $\mathbf{M}(0) = I$  and  $\mathbf{J}(0) = 0$ . The endpoint map  $\phi_t$  is degenerate at  $p_0$  if and only if  $\det(\mathbf{J}(t)) = 0$ .

*Proof:* A sketch of this proof proceeds as follows. Define the smooth map  $\rho: \mathbb{R}^n \rightarrow T_{q_0}^*G$  by

$$\rho(a) = T_{q_0}^*L_{q_0}^{-1}\left(\sum_{i=1}^n a_i P_i\right)$$

and define  $q: [0, 1] \times \mathbb{R}^n \rightarrow G$  by  $q(t, a) = \phi_t \circ \rho(a)$ . Let

$$\eta^j(t, a) = T_{q(t, a)}L_{q(t, a)^{-1}}\left(\frac{\partial q(t, a)}{\partial a_j}\right)$$

for  $j \in \{1, \dots, n\}$ . Define  $\mathbf{J}: [0, 1] \rightarrow \mathbb{R}^{n \times n}$  so that the matrix  $\mathbf{J}(t)$  has entries  $[\mathbf{J}]_{ij} = \eta_i^j(t, a)$ , i.e., the  $j$ th column of  $\mathbf{J}(t)$  is the coordinate representation of  $\eta^j(t, a)$  with respect to  $\{X_1, \dots, X_n\}$ . Given  $p_0 = \rho(a)$  for some  $a \in \mathbb{R}^n$ , it is straightforward to show that  $\phi_t$  is degenerate at  $p_0$  if and only if  $\det(\mathbf{J}(t)) = 0$ .

It remains to show that  $\mathbf{J}(t)$  can be computed as described in the theorem. Define

$$\zeta(t, a) = T_{q(t, a)}L_{q(t, a)^{-1}}\left(\frac{\partial q(t, a)}{\partial t}\right).$$

Taking  $\mu_1(t), \dots, \mu_n(t)$  as coordinates of  $\mu(t)$ , we verify that (4) and (9) are equivalent. We extend each coordinate function to  $\mu_i: [0, 1] \times \mathbb{R}^n \rightarrow \mathbb{R}$ , so  $\mu_i(t, a)$  solves (9) with initial condition  $\mu_i(0, a) = a_i$ . Define  $\mathbf{M}: [0, 1] \rightarrow \mathbb{R}^{n \times n}$  by  $[\mathbf{M}(t)]_{ij} = \partial \mu_i / \partial a_j$ . Our result follows by differentiation, noting that

$$\dot{\eta}^j = \frac{\partial \zeta}{\partial a_j} - [\zeta, \eta^j] = \frac{\partial}{\partial a_j} \frac{\delta h}{\delta \mu} - \left[ \frac{\delta h}{\delta \mu}, \eta^j \right]$$

from Lemma 1 and Theorem 3. ■

### III. APPLICATION TO A PLANAR ELASTIC ROD

The previous section derived coordinate formulae to compute necessary and sufficient conditions for a particular class of optimal control problems on manifolds. Here, we apply these results to a planar elastic rod. Section III-A recalls that the framed curve traced by the rod in static equilibrium is a local solution to a geometric optimal control problem [31], [32]. Section III-B proves that the set of all trajectories that are normal with respect to this problem is a smooth manifold of dimension three that can be parameterized by a single chart (Theorem 6). Section III-C proves that the set of all normal trajectories that are also local optima is an open subset of this smooth manifold, and provides a computational test for membership in this subset (Theorem 7). These two results suffice to describe all possible configurations of the elastic rod that can be achieved by quasi-static manipulation. Section III-E presents a sampling-based planning algorithm for quasi-static manipulation based on these results.

#### A. Model

We model the object in Figure 1 as a planar elastic rod. Assuming it is thin, inextensible, and unit length, we describe the shape of this rod by a continuous map  $q: [0, 1] \rightarrow G$ , where  $G = SE(2)$ . We require this map to satisfy

$$\dot{q} = q(X_1 + uX_3) \quad (12)$$

for some  $u: [0, 1] \rightarrow U$ , where  $U = \mathbb{R}$  and

$$X_1 = \begin{bmatrix} 0 & 0 & 1 \\ 0 & 0 & 0 \\ 0 & 0 & 0 \end{bmatrix} \quad X_2 = \begin{bmatrix} 0 & 0 & 0 \\ 0 & 0 & 1 \\ 0 & 0 & 0 \end{bmatrix} \quad X_3 = \begin{bmatrix} 0 & -1 & 0 \\ 1 & 0 & 0 \\ 0 & 0 & 0 \end{bmatrix}$$

is a basis for  $\mathfrak{g}$ . Denote the dual basis for  $\mathfrak{g}^*$  by  $\{P_1, \dots, P_3\}$ . We refer to  $q$  and  $u$  together as  $(q, u): [0, 1] \rightarrow G \times U$  or simply as  $(q, u)$ . We assume the base of the rod is held fixed at the origin, so that  $q(0) = e$ . The other end is held by a robotic gripper, which we assume can impose arbitrary  $q(1)$ . We denote the space of all  $q(1)$  by  $\mathcal{B} = G$ . For fixed  $q(1)$ , the rod will remain motionless only if its shape locally minimizes total elastic energy. In particular, we say that  $(q, u)$  is in static equilibrium if it is a local optimum of

$$\begin{aligned} & \underset{q, u}{\text{minimize}} && \frac{1}{2} \int_0^1 u^2 dt \\ & \text{subject to} && \dot{q} = q(X_1 + uX_3) \\ & && q(0) = e, \quad q(1) = b \end{aligned} \quad (13)$$

for some  $b \in \mathcal{B}$ .

#### B. Necessary Conditions for Static Equilibrium

*Theorem 5:* Define

$$\mathcal{A} = \{a \in \mathbb{R}^3 : (a_2, a_3) \neq (0, 0)\}.$$

A trajectory  $(q, u)$  is normal with respect to (13) if and only if there exists  $\mu: [0, 1] \rightarrow \mathfrak{g}^*$  that satisfies

$$\dot{\mu}_1 = \mu_2 u \quad \dot{\mu}_2 = -\mu_1 u \quad \dot{\mu}_3 = -\mu_2 \quad (14)$$

$$\dot{q} = q(X_1 + uX_3) \quad (15)$$

$$u = \mu_3 \quad (16)$$

with  $q(0) = e$  and  $\mu(0) = \sum_{i=1}^3 a_i P_i$  for  $a \in \mathcal{A}$ .

*Proof:* We begin by showing that  $(q, u)$  is abnormal if and only if  $u = 0$ . Theorem 1 tells us it is equivalent that  $(q, u)$  is the projection of an integral curve  $(p, q)$  of  $X_H$  that satisfies (2), where  $H(p, q, t) = \widehat{H}(p, q, 0, u(t))$  and

$$\widehat{H}(p, q, 0, u) = \langle p, q(X_1 + uX_3) \rangle.$$

Since  $H$  is left-invariant, the existence of  $(p, q)$  satisfying Theorem 1 is equivalent to the existence of  $\mu$  satisfying the conditions of Theorem 3, namely that

$$\dot{\mu} = \text{ad}_{\delta h / \delta \mu}^* (\mu) \quad \text{and} \quad \dot{q} = q(\delta h / \delta \mu),$$

where  $h = H|_{\mathfrak{g}^*}$ . Application of (9) produces (14)-(15), where we require  $\mu_3 = 0$  to satisfy (2). We therefore have  $\mu_2 = -\dot{\mu}_3 = 0$ , hence also  $\mu_1 u = -\dot{\mu}_2 = 0$ . Since  $\mu$  cannot vanish when  $k = 0$ , we must have  $\mu_1 \neq 0$ , hence  $u = 0$ .

Now, we return to the normal case. Theorem 1 tells us that  $(q, u)$  is normal if and only if it is not abnormal and it is the projection of an integral curve  $(p, q)$  of  $X_H$  that satisfies (2), where  $H(p, q, t) = \widehat{H}(p, q, 1, u(t))$  and

$$\widehat{H}(p, q, 1, u) = \langle p, q(X_1 + uX_3) \rangle - (u^2/2).$$

As before,  $H$  is left-invariant. Application of (9) to the conditions of Theorem 3 produces the same formulae (14)-(15), where (16) follows from (2) because  $\widehat{H}$  is quadratic in  $u$ . It remains to show that trajectories produced by (14)-(16) are not abnormal if and only if  $a \in \mathcal{A}$ . We prove the converse. First, assume  $a \in \mathbb{R}^3 \setminus \mathcal{A}$ , so  $(a_2, a_3) = (0, 0)$ . From (14) and (16), we have  $u = 0$ , hence  $(q, u)$  is abnormal. Now, assume  $(q, u)$  is abnormal, so  $u = 0$ . From (16), we therefore have  $\mu_3 = 0$ , and in particular  $a_3 = 0$ . Plugging this result into (14), we see that  $\mu_2 = -\dot{\mu}_3 = 0$ , hence also that  $a_2 = 0$ . So,  $a \in \mathbb{R}^3 \setminus \mathcal{A}$ . Our result follows. ■

Theorem 5 provides a set of candidates for local optima of (13), which we now characterize. Denote the set of all smooth maps  $(q, u): [0, 1] \rightarrow G \times U$  under the smooth topology by  $C^\infty([0, 1], G \times U)$ . Let  $\mathcal{C} \subset C^\infty([0, 1], G \times U)$  be the subset of all  $(q, u)$  that satisfy Theorem 5. Any such  $(q, u) \in \mathcal{C}$  is completely defined by the choice of  $a \in \mathcal{A}$ , as is the corresponding  $\mu$ . Denote the resulting maps by  $\Psi(a) = (q, u)$  and  $\Gamma(a) = \mu$ . We require three lemmas before our main result (Theorem 7).

*Lemma 3:* If  $\Psi(a) = \Psi(a')$  for  $a, a' \in \mathcal{A}$ , then  $a = a'$ .

*Proof:* Suppose  $(q, u) = \Psi(a)$  and  $\mu = \Gamma(a)$  for some  $a \in \mathcal{A}$ . It suffices to show that  $a$  is uniquely defined by  $u$  (and its derivatives, since  $u$  is clearly smooth). From (14) and (16), we have

$$a_2 = -\dot{\mu}_3(0) = -\dot{u}(0) \quad a_3 = u(0). \quad (17)$$

We differentiate (14) to compute

$$\ddot{u}(0) = a_3 a_1 \quad \ddot{u}(0) = a_2 (a_3^2 - a_1). \quad (18)$$

At least one of these two equations allows us to compute  $a_1$  unless  $(a_2, a_3) = (0, 0)$ , which would violate our assumption that  $a \in \mathcal{A}$ . Our result follows. ■

*Lemma 4:* The map  $\Psi: \mathcal{A} \rightarrow \mathcal{C}$  is a homeomorphism.

*Proof:* The map  $\Psi$  is a bijection—it is well-defined and onto by construction, and is one-to-one by Lemma 3. Continuity of  $\Psi$  follows from Theorem 5. It remains only to show that  $\Psi^{-1}: \mathcal{C} \rightarrow \mathcal{A}$  is continuous—this result is an immediate consequence of (17)-(18). ■

*Lemma 5:* If the topological  $n$ -manifold  $M$  has an atlas consisting of the single chart  $(M, \alpha)$ , then  $N = \alpha(M)$  is a topological  $n$ -manifold with an atlas consisting of the single chart  $(N, \text{id}_N)$ , where  $\text{id}_N$  is the identity map. Furthermore, both  $M$  and  $N$  are smooth  $n$ -manifolds and  $\alpha: M \rightarrow N$  is a diffeomorphism.

*Proof:* Since  $(M, \alpha)$  is chart, then  $N$  is an open subset of  $\mathbb{R}^n$  and  $\alpha$  is a bijection. Hence, our first result is immediate and our second result requires only that both  $\alpha$  and  $\alpha^{-1}$  are smooth maps. For every  $p \in M$ , the charts  $(M, \alpha)$  and  $(N, \text{id}_N)$  satisfy  $\alpha(p) \in N$ ,  $\alpha(M) = N$ , and  $\text{id}_N \circ \alpha \circ \alpha^{-1} = \text{id}_N$ , so  $\alpha$  is a smooth map. For every  $q \in N$ , the charts  $(N, \text{id}_N)$  and  $(M, \alpha)$  again satisfy  $\alpha^{-1}(q) \in M$ ,  $\alpha^{-1}(N) = M$ , and  $\alpha \circ \alpha^{-1} \circ \text{id}_N = \text{id}_N$ , so  $\alpha^{-1}$  is also a smooth map. Our result follows. ■

*Theorem 6:*  $\mathcal{C}$  is a smooth 3-manifold with smooth structure determined by an atlas with the single chart  $(\mathcal{C}, \Psi^{-1})$ .

*Proof:* Since  $\Psi: \mathcal{A} \rightarrow \mathcal{C}$  is a homeomorphism by Lemma 4 and  $\mathcal{A} \subset \mathbb{R}^3$  is open, then  $(\mathcal{C}, \Psi^{-1})$  is a chart whose domain is  $\mathcal{C}$ . Our result follows from Lemma 5. ■

### C. Sufficient Conditions for Static Equilibrium

*Theorem 7:* Let  $(q, u) = \Psi(a)$  and  $\mu = \Gamma(a)$  for some  $a \in \mathcal{A}$ . Define

$$\mathbf{F} = \begin{bmatrix} 0 & \mu_3 & \mu_2 \\ -\mu_3 & 0 & -\mu_1 \\ 0 & -1 & 0 \end{bmatrix} \quad \mathbf{G} = \begin{bmatrix} 0 & 0 & 0 \\ 0 & 0 & 0 \\ 0 & 0 & 1 \end{bmatrix}$$

$$\mathbf{H} = \begin{bmatrix} 0 & \mu_3 & 0 \\ -\mu_3 & 0 & 1 \\ 0 & 0 & 0 \end{bmatrix}.$$

Solve the (linear, time-varying) matrix differential equations

$$\dot{\mathbf{M}} = \mathbf{F}\mathbf{M} \quad \dot{\mathbf{J}} = \mathbf{G}\mathbf{M} + \mathbf{H}\mathbf{J} \quad (19)$$

with initial conditions  $\mathbf{M}(0) = I$  and  $\mathbf{J}(0) = 0$ . Then,  $(q, u)$  is a local optimum of (13) for  $b = q(1)$  if and only if  $\det(\mathbf{J}(t)) \neq 0$  for all  $t \in (0, 1]$ .

*Proof:* As we have already seen, normal extremals of (13) are derived from the parameterized Hamiltonian function

$$\widehat{H}(p, q, 1, u) = \langle p, q(X_1 + uX_3) \rangle - (u^2/2).$$

This function satisfies  $\partial^2 \widehat{H} / \partial u^2 = -1 < 0$  and admits a unique maximum at  $u = \langle p, qX_3 \rangle$ . The maximized Hamiltonian function is

$$H(p, q) = \langle p, qX_1 \rangle + \langle p, qX_3 \rangle^2 / 2.$$

It is clear that  $X_H$  is complete. By Lemma 3, the mapping from  $(q, u)$  to  $a$  and hence to  $\mu = \Gamma(a)$  is unique. By Theorem 3, it is equivalent that the mapping from  $(q, u)$  to  $(p, q)$  is unique. As a consequence, we may apply Theorem 2 to establish sufficient conditions for optimality. Since  $H$

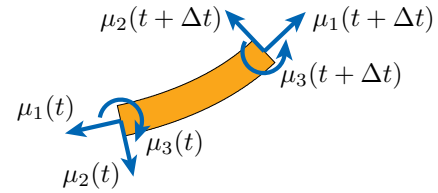


Fig. 2. Forces and torques applied to a piece of the planar elastic rod, providing a physical interpretation of the costate trajectory  $\mu: [0, 1] \rightarrow \mathfrak{g}^*$ . Equilibrium configurations are uniquely defined by the choice of  $a = \mu(0)$ .

is left-invariant, we may apply the equivalent conditions of Theorem 4. Noting that  $h = H|_{\mathfrak{g}^*} \in C^\infty(\mathfrak{g}^*)$  is given by

$$h(\mu) = \mu_1 + \mu_3^2/2,$$

it is easy to verify that  $\mathbf{F}$ ,  $\mathbf{G}$  and  $\mathbf{H}$  take the given form. ■

Theorem 7 provides a computational test of which points  $a \in \mathcal{A}$  actually produce local optima  $\Psi(a) \in \mathcal{C}$  of (13). Let  $\mathcal{A}_{\text{stable}} \subset \mathcal{A}$  be the subset of all  $a$  for which the conditions of Theorem 7 are satisfied and let  $\mathcal{C}_{\text{stable}} = \Psi(\mathcal{A}_{\text{stable}}) \subset \mathcal{C}$ . An important consequence of membership in  $\mathcal{A}_{\text{stable}}$  is smooth local dependence of (13) on variation in  $b$ . Define

$$\mathcal{B}_{\text{stable}} = \{q(1) \in \mathcal{B} : (q, u) \in \mathcal{C}_{\text{stable}}\}$$

and let  $\Phi: \mathcal{C} \rightarrow \mathcal{B}$  be the map taking  $(q, u)$  to  $q(1)$ . Clearly  $\mathcal{A}_{\text{stable}}$  is open, so

$$\Psi|_{\mathcal{A}_{\text{stable}}}: \mathcal{A}_{\text{stable}} \rightarrow \mathcal{C}_{\text{stable}}$$

is a diffeomorphism. We arrive at the following result:

*Theorem 8:* The map  $\Phi \circ \Psi|_{\mathcal{A}_{\text{stable}}}: \mathcal{A}_{\text{stable}} \rightarrow \mathcal{B}_{\text{stable}}$  is a local diffeomorphism.

*Proof:* The map  $\Phi \circ \Psi|_{\mathcal{A}_{\text{stable}}}$  is smooth and by Theorem 7 has non-singular Jacobian  $\mathbf{J}(1)$ . Our result follows from the Implicit Function Theorem [27, Theorem 7.9]. ■

### D. Physical Interpretation of $\mathcal{A}$

The coordinate chart  $\mathcal{A}$  has a physical interpretation. To derive it, we will assume that  $\mu(t)$  describes the force and torque acting on the rod at  $t \in [0, 1]$ , and will show that this assumption allows us to reconstruct (14) and (16). Consider a small piece of the rod (Figure 2). Choose  $(v_1, v_2, \theta)$  so that

$$\begin{bmatrix} \cos \theta & -\sin \theta & v_1 \\ \sin \theta & \cos \theta & v_2 \\ 0 & 0 & 1 \end{bmatrix} = q(t)^{-1}q(t + \Delta t).$$

In static equilibrium, a force and torque balance requires that

$$\begin{aligned} 0 &= -\mu_1(t) + \mu_1(t + \Delta t) \cos \theta - \mu_2(t + \Delta t) \sin \theta \\ 0 &= -\mu_2(t) + \mu_1(t + \Delta t) \sin \theta + \mu_2(t + \Delta t) \cos \theta \\ 0 &= -\mu_3(t) + \mu_3(t + \Delta t) + \mu_1(t + \Delta t) (v_1 \sin \theta \\ &\quad - v_2 \cos \theta) + \mu_2(t + \Delta t) (v_1 \cos \theta + v_2 \sin \theta). \end{aligned}$$

In the limit as  $\Delta t \rightarrow 0$ , we recover (14). Equation (16) then follows from the linear relationship between stress and strain. It is now clear that  $\mathcal{A}$  is a space of forces and torques, and in particular that  $\mu(0) = a \in \mathcal{A}$  describes the force and torque at the base of a planar elastic rod. The reader may also verify that abnormal  $(q, u)$  are exactly those configurations of the rod at which  $\mu(0)$  is indeterminate.

## E. Manipulation Planning

We now know that any equilibrium configuration of a planar elastic rod can be represented by a point in  $\mathcal{A}_{\text{stable}} \subset \mathcal{A} \subset \mathbb{R}^3$  (Theorems 5-7) and that any path of the rod in  $\mathcal{A}_{\text{stable}}$  can be realized by a path of the robotic gripper in  $\mathcal{B}_{\text{stable}}$  (Theorem 8). These results allow us to apply a sampling-based algorithm for manipulation planning (here, we describe one based on PRM [33]):

- Sample points in  $\mathcal{A}$ , for example uniformly at random in  $\{a \in \mathcal{A}: \|a\|_{\infty} \leq w\}$  for some  $w > 0$ . Note that it is possible to choose  $w$  by taking advantage of the correspondence between  $a$  and forces/torques at the base of the elastic rod (Section III-D).
- Keep points that are in  $\mathcal{A}_{\text{stable}}$  and add them as nodes in the roadmap. This test requires only solving the ordinary differential equations (14)-(16) in 3 variables and the matrix differential equations (19) in 18 variables.
- Try to connect each pair of nodes  $a$  and  $a'$  with a straight-line path in  $\mathcal{A}$ , adding this path as an edge in the roadmap if it lies entirely in  $\mathcal{A}_{\text{stable}}$ . This test can be approximated in the usual way by sampling points along the straight-line path at some resolution, again solving (14)-(16) and (19) for each point.
- Declare  $a_{\text{start}}, a_{\text{goal}} \in \mathcal{A}_{\text{stable}}$  to be path-connected if they are connected by a sequence of nodes and edges in the roadmap. This sequence is a continuous and piecewise-smooth map

$$\alpha: [0, 1] \rightarrow \mathcal{A}_{\text{stable}},$$

where  $\alpha(0) = a_{\text{start}}$  and  $\alpha(1) = a_{\text{goal}}$ .

- Move the robotic gripper along the path

$$\Phi \circ \Psi|_{\mathcal{A}_{\text{stable}}} \circ \alpha: [0, 1] \rightarrow \mathcal{B}_{\text{stable}}.$$

This path is again continuous and piecewise-smooth, and can be evaluated at waypoints  $s \in [0, 1]$  by solving the matrix differential equation (15) on  $SE(2)$ .

Each step is trivial to implement using modern numerical methods. It is also easy to include other constraints within this basic framework. For the experiments that we describe in the following section, we check for self-collision (using hierarchical bounding volumes) and enforce bounds on position and orientation of the robotic gripper.

We emphasize that “start” and “goal” for the manipulation planning problem must be points in  $\mathcal{A}_{\text{stable}}$ , or equivalently points in  $\mathcal{C}_{\text{stable}}$  through the diffeomorphism  $\Psi$ . It is insufficient to specify start and goal by points in  $\mathcal{B}_{\text{stable}}$ , since these points do not uniquely define configurations of the rod.

## IV. EXPERIMENTS

### A. Model Validation

Figure 3 shows a comparison between predicted and observed constraint violations—instability, self-collision, and bounds on the position and orientation of the robot holding one end of the rod—in a slice of  $\mathcal{A} \subset \mathbb{R}^3$  on which  $a_3 = -2$  is held constant. The shaded region is the free part  $\mathcal{A}_{\text{free}} \subset \mathcal{A}_{\text{stable}} \subset \mathcal{A}$  of this slice, as predicted by our model.

We found  $\mathcal{A}_{\text{free}}$  by using a two-dimensional continuation method (essentially, by tracing its contour), which was trivial to implement and took less than a minute of computation time on a standard laptop. To test our model, we executed eight straight-line paths  $\alpha: [0, 1] \rightarrow \mathcal{A}$  of the form

$$\alpha(s) = (rs \cos(k\pi/4), rs \sin(k\pi/4), -2)$$

for  $r = 100$  and  $k \in \{0, \dots, 7\}$ . To execute each path in  $\mathcal{A}$ , we moved the robot along the path  $\Phi \circ \Psi \circ \alpha$  in  $\mathcal{B}$ . We terminated execution when a constraint violation was observed to occur in experiment. Figure 3 indicates whether this violation was due to instability, self-collision, or bounds on the robot workspace. There appears to be a good correspondence between theory and experiment, although this correspondence has not yet been made quantitative (e.g., by a measure of sum-squared difference between predicted and observed shapes of the rod). Sources of error include non-uniform modulus of elasticity along the metal strip, uncertainty in the length of this strip, uncertainty in the position and orientation of each endpoint, and plasticity. All of these possibilities raise questions for future work—e.g., planning algorithms that maximize a measure of distance to constraint violation, online calibration to determine physical parameters, vision-based feedback control, etc.

### B. Example of a Planned Path

Figure 4 shows an example of quasi-static manipulation that was planned by our sampling-based algorithm. Notice that the start and goal configurations are both associated with the same boundary conditions, each one being a different local minimum of total elastic energy, i.e., a different local optima  $a_{\text{start}}, a_{\text{goal}} \in \mathcal{A}_{\text{stable}}$  of (13) for the same choice of  $b \in \mathcal{B}_{\text{stable}}$ . The motion shown in Figure 4 therefore does not correspond to a single straight-line path in  $\mathcal{B}_{\text{stable}}$ , where planning has traditionally been done (e.g., [1], [2]). However, this motion does indeed correspond to a single straight-line path in  $\mathcal{A}_{\text{stable}}$  and was trivial to generate with our planning algorithm. We have not yet performed comprehensive experiments that compare our sampling-based algorithm to others in terms of running time, failure probability, etc.—these experiments are a topic of ongoing work. However, we note that a number of planning heuristics like lazy collision-checking [34]—which bring huge speed-ups in practice—are easy to apply when planning in  $\mathcal{A}_{\text{stable}}$  but hard to apply when planning in  $\mathcal{B}_{\text{stable}}$ . Also, should we still want to plan in  $\mathcal{B}_{\text{stable}}$  (i.e., to connect nearby configurations by straight-line paths in  $\mathcal{B}_{\text{stable}}$  rather than in  $\mathcal{A}_{\text{stable}}$ ), it is now easy to do so by using the Jacobian matrix  $\mathbf{J}(1)$ , which is non-singular in  $\mathcal{B}_{\text{stable}}$  by construction. In particular, we have the relationship  $\delta b = \mathbf{J}(1)\delta a$ , which can be inverted to move along straight lines in  $\mathcal{B}_{\text{stable}}$ . Without this relationship, we would be forced to apply gradient descent in the infinite-dimensional space of inputs  $u: [0, 1] \rightarrow U$ , prompting methods of approximation like the one described in [2]. In any case, our key insight was realizing that the set of equilibrium configurations has dimension three—at that point, nearly any planning algorithm will perform well.

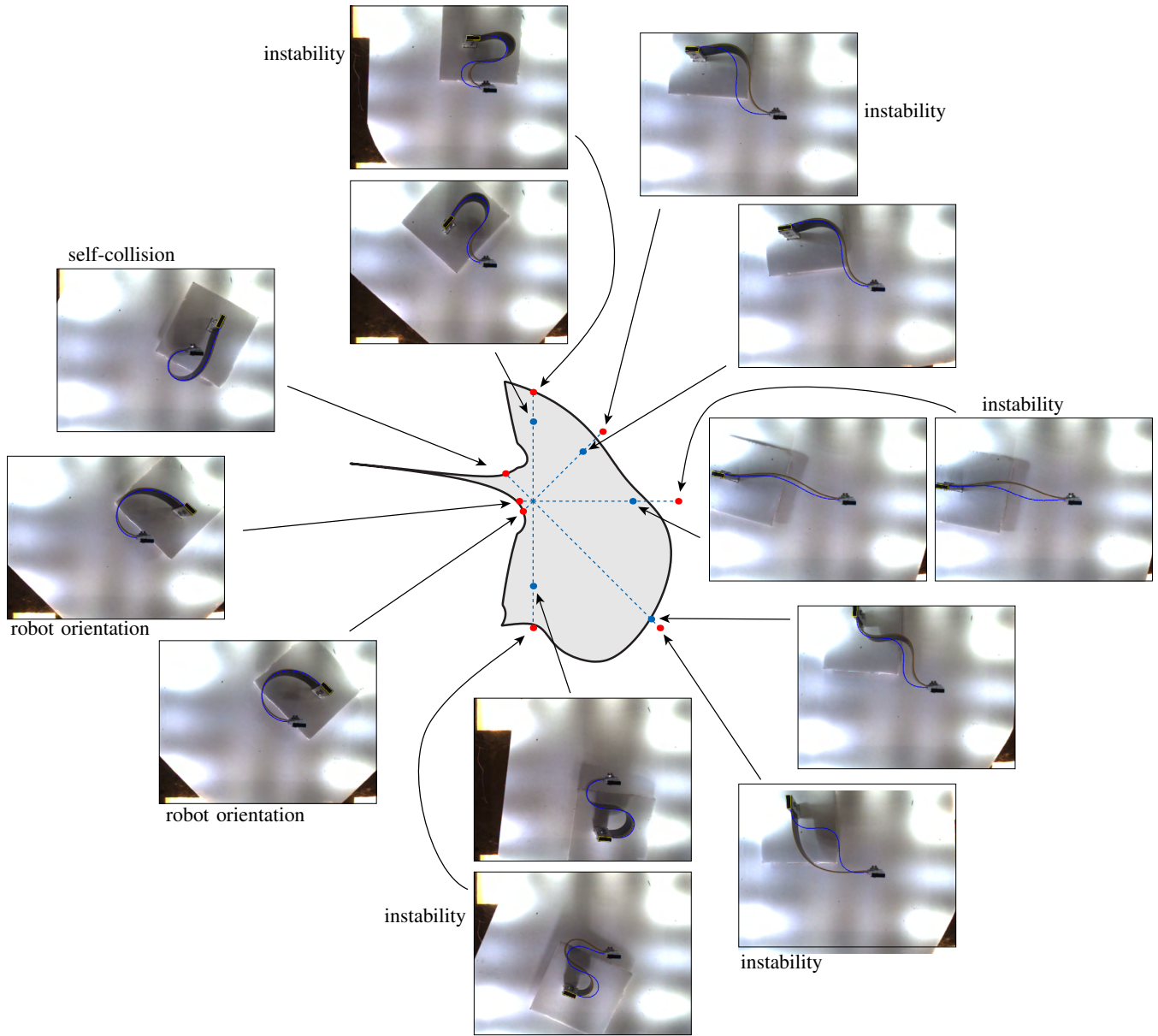


Fig. 3. Comparison between predicted and observed constraint violations—instability, self-collision, and bounds on the position and orientation of the robot holding one end of the rod—in a slice of  $\mathcal{A} \subset \mathbb{R}^3$  on which  $a_3 = -2$  is held constant. The shaded region is the free part  $\mathcal{A}_{\text{free}} \subset \mathcal{A}_{\text{stable}} \subset \mathcal{A}$  of this slice, which has a single connected component. The blue lines are straight-line paths in  $\mathcal{A}$  along which the rod moves, as implemented by the corresponding path in  $\mathcal{B}$ . The blue dots are configurations just before a constraint violation occurred. The red dots are configurations just after one occurred.

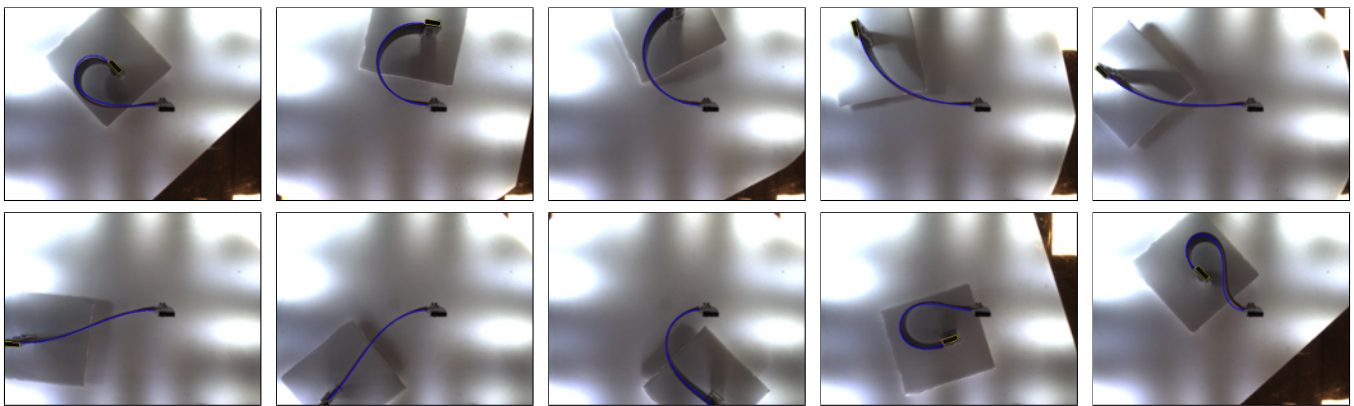


Fig. 4. An example of quasi-static manipulation planned by our sampling-based algorithm. Notice that the robot begins and ends in the same position and orientation. Remarkably, this motion corresponds to a single straight-line path in the global coordinate chart  $\mathcal{A}$  that we derived in Section III.

## V. CONCLUSION

We showed that the set of equilibrium configurations for a planar elastic rod that has a fixed base and that is held at the other end by a robotic gripper is a smooth manifold of dimension three that can be parameterized by a single (global) coordinate chart. This result led to a simple algorithm for manipulation planning. This algorithm was validated with hardware experiments in which the “rod” was a strip of metal being manipulated by an industrial robot.

A straightforward extension is to perform comprehensive experiments that compare our sampling-based algorithm for manipulation planning to others (e.g., [2]) in terms of standard metrics like running time and failure probability. Our approach also extends directly to the spatial case, where the rod is not confined to a plane [35]. Many other generalizations are possible—for example, consideration of gravity or of extensible rods would change only the cost function in (13), i.e., the measure of total energy. Consideration of forces arising from interaction between different parts of the rod (e.g., self-collision) may be much harder. One problem we have not addressed is the identification of physical parameters (e.g., variable stiffness along the rod) from observations of equilibrium configurations. This problem can be cast as inverse optimal control (e.g., as in [36]). The structure established by Theorem 6 allows us to define an orthogonal distance between  $\mathcal{C}$  and these observations, similar to [37], and may lead to an efficient solution.

## ACKNOWLEDGMENTS

Thanks to Z. McCarthy, S. Hutchinson, and D. Shimamoto for helpful discussion. This work was supported by the National Science Foundation (CPS-0931871, CMMI-0956362).

## REFERENCES

- [1] F. Lamiraux and L. E. Kavraki, “Planning paths for elastic objects under manipulation constraints,” *International Journal of Robotics Research*, vol. 20, no. 3, pp. 188–208, 2001.
- [2] M. Moll and L. E. Kavraki, “Path planning for deformable linear objects,” *IEEE Trans. Robot.*, vol. 22, no. 4, pp. 625–636, Aug. 2006.
- [3] Y. Sachkov, “Maxwell strata in the euler elastic problem,” *Journal of Dynamical and Control Systems*, vol. 14, no. 2, pp. 169–234, 04 2008.
- [4] —, “Conjugate points in the euler elastic problem,” *Journal of Dynamical and Control Systems*, vol. 14, no. 3, pp. 409–439, 07 2008.
- [5] A. A. Agrachev and Y. L. Sachkov, *Control theory from the geometric viewpoint*. Berlin: Springer, 2004, vol. 87.
- [6] J. E. Hopcroft, J. K. Kearney, and D. B. Krafft, “A case study of flexible object manipulation,” *The International Journal of Robotics Research*, vol. 10, no. 1, pp. 41–50, 1991.
- [7] J. Takamatsu, T. Morita, K. Ogawara, H. Kimura, and K. Ikeuchi, “Representation for knot-tying tasks,” *IEEE Trans. Robot.*, vol. 22, no. 1, pp. 65–78, Feb. 2006.
- [8] H. Wakamatsu, E. Arai, and S. Hirai, “Knotting/unknotted manipulation of deformable linear objects,” *The International Journal of Robotics Research*, vol. 25, no. 4, pp. 371–395, 2006.
- [9] M. Saha and P. Ito, “Manipulation planning for deformable linear objects,” *IEEE Trans. Robot.*, vol. 23, no. 6, pp. 1141–1150, Dec. 2007.
- [10] M. Bell and D. Balkcom, “Knot tying with single piece fixtures,” in *Int. Conf. Rob. Aut.*, May 2008.
- [11] H. Inoue and H. Inaba, “Hand-eye coordination in rope handling,” in *ISRR*, 1985, pp. 163–174.
- [12] J. van den Berg, S. Miller, K. Goldberg, and P. Abbeel, “Gravity-based robotic cloth folding,” in *WAFR*, 2011.
- [13] Q. Lin, J. Burdick, and E. Rimon, “A stiffness-based quality measure for compliant grasps and fixtures,” *IEEE Trans. Robot. Autom.*, vol. 16, no. 6, pp. 675–688, Dec. 2000.
- [14] K. Gopalakrishnan and K. Goldberg, “D-space and deform closure grasps of deformable parts,” *International Journal of Robotics Research*, vol. 24, no. 11, pp. 899–910, Nov. 2005.
- [15] Y. Asano, H. Wakamatsu, E. Morinaga, E. Arai, and S. Hirai, “Deformation path planning for manipulation of flexible circuit boards,” in *IEEE/RSJ Int. Conf. Int. Rob. Sys.*, Oct. 2010.
- [16] R. Jansen, K. Hauser, N. Chentanez, F. van der Stappen, and K. Goldberg, “Surgical retraction of non-uniform deformable layers of tissue: 2d robot grasping and path planning,” in *IEEE/RSJ Int. Conf. Int. Rob. Sys.*, Oct. 2009, pp. 4092–4097.
- [17] N. M. Amato and G. Song, “Using motion planning to study protein folding pathways,” *Journal of Computational Biology*, vol. 9, no. 2, pp. 149–168, 2002.
- [18] J. H. Solomon and M. J. Z. Hartmann, “Extracting object contours with the sweep of a robotic whisker using torque information,” *Int. J. Rob. Res.*, vol. 29, no. 9, pp. 1233–1245, 08 2010.
- [19] H. Tanner, “Mobile manipulation of flexible objects under deformation constraints,” *IEEE Trans. Robot.*, vol. 22, no. 1, pp. 179–184, Feb. 2006.
- [20] G. S. Chirikjian and J. W. Burdick, “The kinematics of hyper-redundant robot locomotion,” *IEEE Trans. Robot. Autom.*, vol. 11, no. 6, pp. 781–793, Dec. 1995.
- [21] D. C. Rucker, R. J. Webster, G. S. Chirikjian, and N. J. Cowan, “Equilibrium conformations of concentric-tube continuum robots,” *Int. J. Rob. Res.*, vol. 29, no. 10, pp. 1263–1280, 09 2010.
- [22] A. Shkolnik and R. Tedrake, “Path planning in 1000+ dimensions using a task-space voronoi bias,” in *Int. Conf. Rob. Aut.*, Kobe, Japan, May 2009, pp. 2061–2067.
- [23] G. Chirikjian and J. Burdick, “A modal approach to hyper-redundant manipulator kinematics,” *IEEE Trans. Robot. Autom.*, vol. 10, no. 3, pp. 343–354, Jun. 1994.
- [24] A. De Luca, R. Mattone, and G. Oriolo, “Steering a class of redundant mechanisms through end-effector generalized forces,” *IEEE Trans. Robot. Autom.*, vol. 14, no. 2, pp. 329–335, Apr. 1998.
- [25] Z. McCarthy and T. Bretl, “Mechanics and manipulation of planar elastic kinematic chains,” in *IEEE Int. Conf. Rob. Aut.*, St. Paul, MN, May 2012.
- [26] L. S. Pontryagin, V. G. Boltyanskii, R. V. Gamkrelidze, and E. F. Mishchenko, *The Mathematical Theory of Optimal Processes*. John Wiley, 1962.
- [27] J. M. Lee, *Introduction to smooth manifolds*. New York: Springer, 2003, vol. 218.
- [28] J. E. Marsden and T. S. Ratiu, *Introduction to mechanics and symmetry: a basic exposition of classical mechanical systems*, 2nd ed. New York: Springer, 1999.
- [29] R. Murray, Z. X. Li, and S. Sastry, *A Mathematical Introduction to Robotic Manipulation*. Boca Raton, FL: CRC Press, 1994.
- [30] A. Bloch, P. Krishnaprasad, J. Marsden, and T. Ratiu, “The Euler-Poincaré equations and double bracket dissipation,” *Communications In Mathematical Physics*, vol. 175, no. 1, pp. 1–42, Jan. 1996.
- [31] J. Biggs, W. Holderbaum, and V. Jurdjevic, “Singularities of optimal control problems on some 6-d lie groups,” *IEEE Trans. Autom. Control*, vol. 52, no. 6, pp. 1027–1038, June 2007.
- [32] G. Walsh, R. Montgomery, and S. Sastry, “Optimal path planning on matrix lie groups,” in *IEEE Conference on Decision and Control*, vol. 2, Dec. 1994, pp. 1258–1263.
- [33] L. E. Kavraki, P. Svetska, J.-C. Latombe, and M. Overmars, “Probabilistic roadmaps for path planning in high-dimensional configuration spaces,” *IEEE Trans. Robot. Autom.*, vol. 12, no. 4, pp. 566–580, 1996.
- [34] G. Sánchez and J.-C. Latombe, “On delaying collision checking in PRM planning: Application to multi-robot coordination,” *Int. J. Rob. Res.*, vol. 21, no. 1, pp. 5–26, 2002.
- [35] T. Bretl and Z. McCarthy, “Equilibrium configurations of a Kirchhoff elastic rod under quasi-static manipulation,” in *Workshop on the Algorithmic Foundations of Robotics*, Boston, MA, Jun. 2012.
- [36] S. Javdani, S. Tandon, J. Tang, J. F. O’Brien, and P. Abbeel, “Modeling and perception of deformable one-dimensional objects,” in *Int. Conf. Rob. Aut.*, Shanghai, China, May 2011.
- [37] A. Keshavarz, Y. Wang, and S. Boyd, “Imputing a convex objective function,” in *IEEE Multi-Conference on Systems and Control*, Sep. 2011.